Visualization on the Riemann sphere of Schröder iteration functions and their efficient computation

V. DRAKOPOULOS

Department of Informatics, Theoretical Informatics,
University of Athens,
Panepistimioupolis 157 71, Athens,
GREECE
email: vasilios@di.uoa.gr

S. GEORGIOU

Department of Mathematics,
University of Athens,
Panepistimioupolis 157 84, Athens,
GREECE
email: sgeorg@math.uoa.gr

Abstract: - The theory of Julia and Fatou holds for the complex plane as well as for the Riemann sphere, with minor modifications. The latter space seems a more natural approach to examine rational functions. Schröder iteration functions, a generalization of Newton-Raphson method to determine roots of equations, are generally rational functions which, until now, are examined only in the complex plane. On the Riemann sphere we examine the Julia sets of the Schröder functions constructed to converge to the nth roots of unity and the orbits of all free critical points of these functions as applied to a one-parameter family of cubic polynomials. Finally, we present a new algorithmic construction to maximize the computational efficiency of the Schröder functions.

Key-Words: - critical point, Fatou set, Julia set, Riemann sphere, Schröder's method

1 Introduction

The method of iteration is the prototype of all numerical methods for attacking the problem of solving (nonlinear) equations in one and several variables. The convergence of these methods, generally, depends upon the initial approximation to a root of our equation. In the special case of polynomial equations, good a priori knowledge of the desired root of the equation often is not available. Looking at the set of all the starting values from a geometrical point of view will definitely help us to choose these initial approximations to a root and compare the convergence properties of various iterative methods.

Ernst Schröder [9] in 1870 described a method of finding a rational iterating function of any desired "order of convergence" to determine roots of equations. For polynomial equations this involves the iteration of rational functions over the complex Riemann sphere which is described by the classical theory of Julia [8] and Fatou [6] and its subsequent developments, also of paramount importance in the context of Numerical Analysis. In what follows we abbreviate as f^k the k-fold composition $f \circ f \circ \cdots \circ f$, by *region* we mean a connected open set on the *extended complex plane* $\overline{\mathbb{C}} = \mathbb{C} \cup \{\infty\}$ and if we have a rational function of the form $R(z) = P(z)/Q(z)$, where $P(z)$ and $Q(z)$ are complex polynomials with no common factors, the *degree* of R is defined by $\deg(R) = \max\{\deg(P), \deg(Q)\}$.

It appears that convergence of the sequence of iterates $z_0, R(z_0), R^2(z_0), \ldots$ is assured for every

choice of starting point z_0 on the extended complex plane, except when z_0 is a point of a certain nowhere dense perfect set, the Julia set $J(R)$. How "close" a starting point must be to the desired root depends on certain convergence conditions and how "fast" does the method converge depends on the order of convergence of our iterative method.

It may happen, however, that when choosing a starting point z_0 in a certain domain, convergence takes place not to a zero of our polynomial, but to a *periodic orbit* or *cycle*, that is a set of $p \geq 2$ distinct points $\{a_1, \ldots, a_p\}$ such that

$$R(a_1) = a_2, \ldots, R(a_{p-1}) = a_p, R(a_p) = a_1,$$

so that, in fact, for each $k = 1, 2, \ldots, p$, $z = a_k$ is a solution of $R^p(z) = z$. Hence, a point a is *periodic* if $R^p(a) = a$ for some $p > 0$; it is *repelling, indifferent* or *attracting* depending on whether $|(R^p)'(a)|$ is greater than, equal to, or less than one. If $|(R^p)'(a)| = 0$, a is termed *superattracting*. If $p = 1$, z is called a *fixed point* of R. The *Julia set* $J(R)$ of a rational function R is the closure of all repelling periodic points of R and the *Fatou set* is its complement on $\overline{\mathbb{C}}$. Also, if a is an attracting fixed point of R then

$$A(a) = \{z \in \overline{\mathbb{C}} : \lim_{k \to \infty} R^k(z) = a\}$$

is the *basin of attraction* of a. We also have the following important property: the boundary of $A(a)$ is $J(R)$. It follows that if R has several distinct attracting fixed points, then their basins of attraction share the same boundary, the Julia set of R.

A portion of this paper was motivated by [5] and could be considered an extension of it to the Riemann sphere. We first outline the construction of the extended complex plane as a sphere. Then, we maximize the computational efficiency of the Schröder functions by reconstructing them. Finally we examine on the Riemann sphere, with the aid of microcomputer-generated plots, the Julia sets of the Schröder scheme as applied to the set of functions $f_n(z) = z^n - 1$ for $n = 2, 3, \ldots$, their roots' basins of attraction and the dynamics of Schröder maps applied to the one-parameter family of cubic polynomials presented in [2].

2 Schröder Iteration Functions revisited

Schröder iteration functions are a family of rational iteration functions which are designed to converge with order $\sigma \geq 2$ to the zeros of a function f. We define the *Schröder iteration functions* as (see [7])

$$S_\sigma(z) = z + \sum_{k=1}^{\sigma-1} c_k(z)[-f(z)]^k, \quad \sigma = 2, 3, \ldots, \quad (1)$$

where

$$c_k(z) = \frac{1}{k!}\left[\frac{1}{f'(z)}\frac{d}{dz}\right]^{k-1}\frac{1}{f'(z)}$$

and

$$\left[\frac{1}{f'(z)}\frac{d}{dz}\right]^{k-1} = \underbrace{\left[\frac{1}{f'(z)}\frac{d}{dz}\right]\left[\frac{1}{f'(z)}\frac{d}{dz}\right]\cdots\left[\frac{1}{f'(z)}\frac{d}{dz}\right]}_{k-1 \text{ factors}}.$$

The coefficients $c_k(z)$ are analytic functions in every subregion T of $\mathbb{C}$ for $f'(z) \neq 0$. For $\sigma = 2$, we get the familiar Newton–Raphson function

$$S_2(z) = N(z) = z - f(z)/f'(z).$$

We observe that Schröder's iteration is Newton–Raphson-like in form. The iteration sequence $z_{n+1} = S_\sigma(z_n), \sigma = 2, 3, \ldots$, converges locally to the roots z_i^*, $i = 1, 2, \ldots, \deg(f)$, of $f(z) = 0$, as $O(|z_n - z_i^*|^\sigma)$ ([7], Theorem 6.12c, p. 530). The S_σ are truncations of a general infinite series in f and it is easily seen that their construction requires the first $\sigma - 1$ derivatives of f. Thus, the above form of Eq. (1) is not so useful for generalized computations and programming of all the S_σ terms. To eliminate this inconvenience we deem it necessary to introduce the following construction.

Starting with $h_1(z) = 1$ we have

$$\left(\frac{h_1(z)}{f'(z)}\right)'\frac{1}{f'(z)} = \frac{h_2(z)}{[f'(z)]^3},$$

$$\left(\frac{h_2(z)}{[f'(z)]^3}\right)'\frac{1}{f'(z)} = \frac{h_3(z)}{[f'(z)]^5}$$

and, in general,

$$h_{k+1}(z) = h_k'(z)f'(z) - (2k-1)h_k(z)f''(z) \quad (2)$$

for $k = 1, 2, \ldots, \sigma - 2$. Thus,

$$c_k(z) = \frac{1}{k!} \frac{h_k(z)}{[f'(z)]^{2k-1}},$$

and Eq. (1) becomes

$$S_\sigma(z) = z + \sum_{k=1}^{\sigma-1} \frac{(-1)^k}{k!} \frac{h_k(z)}{[f'(z)]^{2k-1}} [f(z)]^k. \qquad (3)$$

We observe that S_σ uses $\sigma - 1$ number of h_k, $k = 1, 2, \ldots, \sigma - 1$, and $\sigma \geq 2$.

For $\sigma = 2$, the fixed point condition $S_\sigma(z) = z$ implies that $f(z) = 0$. For $\sigma > 2$, it implies that $f(z) = 0$, or

$$\sum_{k=1}^{\sigma-1} \frac{(-1)^{k-1}}{k!} \frac{h_k(z)}{[f'(z)]^{2k-1}} [f(z)]^{k-1} = 0. \qquad (4)$$

We shall refer to the zeros of Eq. (4) as *extraneous fixed points*. Their appearance may complicate the root-finding procedure. For more informations about the behaviour of these points and specifically for the attracting ones which lead to pathological cycles, we refer to [3].

Suppose that f is a polynomial of degree $d \geq 2$ and that its first σ derivatives exist. Then $h_k, k = 1, 2, \ldots, \sigma$, are polynomials and S_σ are rational functions. The Julia–Fatou theory can describe the possible types of behavior of the iteration sequence $(S_\sigma^n)_{n=1}^\infty$. To analyze this behavior, the critical points of S_σ will play a crucial role.

Critical values of a function f are defined as those values $v \in \mathbb{C}$ for which $f(z) = v$ has a multiple root. The multiple root $z = c$ is called the *critical point* of f. This is equivalent to the condition $f'(c) = 0$. The underlying reason for studying these special orbits rests in the following theorem of Fatou [6]:

Theorem 1 *If R is a rational function having an attracting cycle, then at least one critical point will converge to it.*

Among the critical points of S_σ determined by the condition $S'_\sigma(z) = 0$ are the zeros z_i^* which are also attracting fixed points of the S_σ. These points are obviously not free to converge to any other attracting cycles. Other roots, which we shall call the *free critical points*, are available, however.

Differentiating Eq. (3) with respect to z we have that the condition $S'_\sigma(z) = 0$ implies that

$$h_\sigma(z)[f(z)]^{\sigma-1} = 0. \qquad (5)$$

Thus, the free critical points of S_σ are the zeros of h_σ.

3 Computational Techniques

The *computational efficiency* of an iterative method is a measure of how much computation must be done to arrive at a given accuracy in a root. Because the computational efficiency of Schröder's method depends upon the number of evaluations of f and its derivatives, we describe here how one can reduce these calculations and produce quickly all of the S_σ terms.

If we denote as

$$\Phi_k(z) = \frac{(-1)^k}{k!} h_k(z), \quad k = 1, 2, \ldots, \sigma - 1,$$

Eq. (3) becomes

$$S_\sigma(z) = z + \frac{\Phi_1(z)}{f'(z)} f(z) + \frac{\Phi_2(z)}{[f'(z)]^3} [f(z)]^2 + \cdots + \frac{\Phi_{\sigma-1}(z)}{[f'(z)]^{2\sigma-3}} [f(z)]^{\sigma-1}.$$

We define as

$$F(z) = f(z)/f'(z) \text{ and } G(z) = f(z)/[f'(z)]^2, \quad (6)$$

therefore

$$S_\sigma(z) = z + (\Phi_1(z) + (\Phi_2(z) + \cdots + \Phi_{\sigma-1}(z)G(z))G(z))F(z). \qquad (7)$$

During the development of the images we compute the coefficients of the polynomials f', Φ_k, $k = 1, 2, \ldots, \sigma - 1$, before the main pixel-scanning procedure begins. In the pixel-scanning procedure, for each iteration of a point z_n, we compute, $f(z_n)$ and $f'(z_n)$ with Horner's scheme, $F(z_n)$ and $G(z_n)$ from (6) and $S_\sigma(z_n)$ from (7).

The case of the λ-parameter space of the cubic polynomials

$$p_\lambda(z) = z^3 + (\lambda - 1)z - \lambda = (z - 1)(z^2 + z + \lambda), \quad \lambda \in \mathbb{C}, \qquad (8)$$

which will be described in Section 6, involves greater difficulty because the coefficients of the polynomials f' and Φ_k depend on the parameter λ that changes for each pixel. So, f' and Φ_k must be computed from the beginning for each pixel in the scanning procedure. Something like that is time-consuming: one Φ_k is evaluated recursively from the $h_k, k = 1, 2, \ldots, \sigma - 1$, and in every iteration we apply Eq. (2). In this case, the initial evaluation of Φ_k takes place in a symbolic way; that is, the information for the creation of each coefficient of the polynomial Φ_k is stored according to the parameter λ. Fortunately, we have to multiply only a number (independently of λ) by a specific power of $\lambda - 1$. That can be seen from the following.

Let $c_i, i = 1, 2, \ldots$, be complex numbers independent of λ or of $a = \lambda - 1$ and not excluding the case where some of them are equal. Note that h_k are the polynomials presented in Section 2. We then have

$$\begin{aligned} p_\lambda(z) &= z^3 + az - \lambda \\ p'_\lambda(z) &= c_1 z^2 + a \\ p''_\lambda(z) &= c_2 z \end{aligned}$$

and we define

$$\begin{aligned} q(z) &= z^3 + z - 1 \\ q'(z) &= c_1 z^2 + 1 \\ q''(z) &= c_2 z. \end{aligned}$$

For the h_k associated with q' and q'' we have that

$$\begin{aligned} h_1(z) &= 1 \\ h_2(z) &= c_2 z \\ h_3(z) &= c_3 z^2 + c_4 \\ h_4(z) &= c_5 z^3 + c_6 z \end{aligned}$$

and so on. To compute the coefficients of the polynomial $h_k(z)$ associated with p'_λ and p''_λ we modify the above mentioned $h_k(z)$ for $k = 1, 2, \ldots, \sigma - 1$ so that

$$\begin{aligned} h_1(z) &= 1 \\ h_2(z) &= c_2 z \\ h_3(z) &= c_3 z^2 + c_4 a \\ h_4(z) &= c_5 z^3 + c_6 a z \end{aligned}$$

and so on. The above analysis of h_k, $k = 1, 2, \ldots, \sigma - 1$, generally gives that

$$h_k(z) = \sum_{i=0}^{m} c_i a^i z^{k-1-2i},$$

where $m = (k-1)/2$ if k is odd and $m = (k/2) - 1$ if k is even. It is obvious from the above that one of the roots of $h_k(z) = 0$, for even values of k, is $z = 0$. Thus, if σ is even, the map $S_\sigma(p_\lambda(z))$ has $z = 0$ as a free critical point.

4 The World is Round

To obtain a metric on $\overline{\mathbb{C}}$ we identify $\mathbb{C}$ with the horizontal plane $\{(x_1, x_2, x_3) \in \mathbb{R}^3 : x_3 = 0\}$ in $\mathbb{R}^3$ and proceed to construct the usual model for $\overline{\mathbb{C}}$ as a sphere.

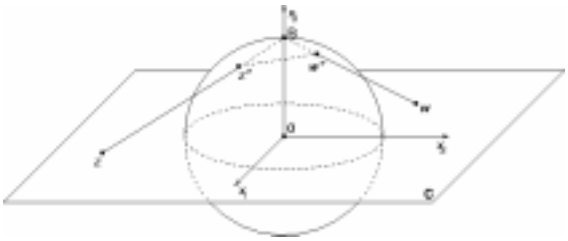

Figure 1: Stereographic projection

Let S be the sphere in $\mathbb{R}^3$ with unit radius and centre at the origin so that $\mathbb{C}$ cuts S along the equator, that is

$$S = \{(x_1, x_2, x_3) \in \mathbb{R}^3 : x_1^2 + x_2^2 + x_3^2 = 1\}$$

and denote the point $(0, 0, 1)$ (the top point of S) by B. This point is called the *north pole*. Another choice is to take the south pole at the origin. We now project each point $z \in \mathbb{C}$ linearly towards (or away from) B until it meets S at a point z^* distinct from B: this means that a line from B to a point z in the complex plane intersects the sphere at a point z^*. If $|z| > 1$ then z^* is in the northern hemisphere and if $|z| < 1$ then z^* is in the southern hemisphere; also for $|z| = 1$, $z^* = z$. The map $\pi : z \mapsto z^*$ is called the *stereographic projection* of $\mathbb{C}$ into S. We may equivalently define $\pi : S \setminus \{B\} \to \mathbb{C}$ with $\pi(x_1, x_2, x_3) = (x_1 + ix_2)/(1 - x_3)$. Clearly, if $|z|$ is 'large', then z^* is 'near' to B and with this in mind we define the projection $\pi(\infty)$ of ∞ to be B. This mapping is *conformal* (i.e., angle-preserving), and so the corresponding conformal geometries are the same. With this definition, the identification of $\overline{\mathbb{C}}$ with S allows us to use them interchangeably, because π is a bijective map from $\overline{\mathbb{C}}$ to S, and this

explains why $\overline{\mathbb{C}}$ is also called the *Riemann sphere*: see Figure 1.

We now use the bijection π of $\overline{\mathbb{C}}$ onto S to transfer the Euclidean metric (in $\mathbb{R}^3$) from S to a metric χ on $\overline{\mathbb{C}}$: this simply means that χ is defined in the natural way by the formula

$$\chi(z,w) = |\pi(z) - \pi(w)| = |z^* - w^*|.$$

A gentle exercise in Vector Geometry (which we omit) yields an explicit formula for χ, namely

$$\chi(z,w) = \frac{2|z-w|}{\sqrt{(1+|z|^2)(1+|w|^2)}}$$

when z and w are in $\mathbb{C}$, while for z in $\mathbb{C}$,

$$\chi(z,\infty) = \lim_{w\to\infty} \chi(z,w) = \frac{2}{\sqrt{(1+|z|^2)}}.$$

As $\chi(z,w)$ is the Euclidean length of the chord joining z^* to w^*, χ is called the *chordal metric* on $\overline{\mathbb{C}}$.

5 Julia Sets of Schröder Functions applied to the Polynomials $f_n(z) = z^n - 1$ and their Zeros' Basins of Attraction

In [5] we examined in the complex plane the Julia sets of Schröder functions S_σ, for $\sigma = 2, 3, \ldots$, constructed to converge to the nth roots of unity and these roots' basins of attraction. We have furthered this by examining the above mentioned sets on the Riemann sphere. With this projection the outcome is even more astonishing and useful than the usual examination in the complex plane.

The projection of the image on the Riemann sphere can be accomplished after three fundamental steps: firstly, we project our grid upon the Riemann sphere, secondly, we project the sphere on the plane using the stereographic projection described in Section 4 and, thirdly, we produce the basin of attraction or the Julia set. The first step can be accomplished by employing the *normal projection* according to [1] and observing the sphere from the south pole. The second step uses the fact that the interior of the south hemisphere is mapped to the interior of a large disk around the origin. The third step was computed by almost the same algorithm as described in Section 4 of [5], except that we did not take a square as our starting value's grid, but a circle.

We observe that, for a given polynomial f_n, the complexity of the basin maps increases with the order σ of the S_σ maps and with each increment a new set of n "petals" appears to be embedded in an infinitely self-similar fashion. To have an idea how this looks like on the sphere, we can rotate it using the *width* and *length angles* assigned to our program. First the y-rotation takes place and then the x-rotation.

The white regions in some of the figures, are not to be interpreted as part of a basin of attraction $A(z^*)$. Since $f_n'(0) = 0$, $z = 0$ is mapped to *the point at infinity*. Points near $z = 0$ may first be mapped many orders of magnitude away from it, whereupon a great number of iterations might be required to bring them back to the z_i^*, if at all. Therefore, these grid points would remain as part of the background which has been plotted as white. We can control these white regions with an *overflow* parameter added to the program for this special dynamic behaviour. Analysis of these plots that considers individually each iteration procedure S_σ as applied to f_n appears in [4]. For the Figures 2 to 4 the angles were, in the x-direction, $O°$ and, in the y-direction, $3O°$. The overflow parameter was $1E10$ for $n = 2, 3$ and $1E13$ for $n = 4$.

Case 1. $\sigma = 2$: The basins of attraction for $n = 2, 3$ are presented in Figures 2(a), 3(a), respectively. The Julia set for $n = 4$ is presented in Figure 4(a).

(a) (b) (c)

Figure 2: Schröder basins of attraction for the roots of $f_2(z) = z^2 - 1$ on the Riemann sphere. Blue regions constitute $A(1)$; yellow regions constitute $A(-1)$; (a) S_2 method, (b) S_3 method, (c) S_4 method.

Case 2. $\sigma = 3$: The basins of attraction for $n = 2, 3$ are presented in Figures 2(b), 3(b), respectively. The Julia set for $n = 4$ is presented in Figure 4(b).

Case 3. $\sigma = 4$: The basins of attraction for $n =$

(a) (b) (c)

Figure 3: Schröder basins of attraction for the roots of $f_3(z) = z^3 - 1$ on the Riemann sphere. Blue regions constitute $A(1)$; yellow regions constitute $A(-0.5 + i\,0.5\sqrt{3})$; green regions constitute $A(-0.5 - i\,0.5\sqrt{3})$. (a) S_2 method, (b) S_3 method, (c) S_4 method.

2, 3 are presented in Figures 2(c), 3(c), respectively. The Julia set for $n = 4$ is presented in Figure 4(c).

(a) (b) (c)

Figure 4: Julia sets of the Schröder functions applied to $f_4(z) = z^4 - 1$ on the Riemann sphere. (a) S_2 method, (b) S_3 method, (c) S_4 method.

6 A Walk in Parameter Space

We now focus attention on Schröder iteration methods associated with the particular one parameter family of cubic polynomials (9) the zeros of which are $z_1^* = 1$, $z_2^* = (-1 + \sqrt{1 - 4\lambda})/2$ and $z_3^* = (-1 - \sqrt{1 - 4\lambda})/2$.

Note the λ-dependence of z_2^* and z_3^*. The polynomials p_λ are exactly the monic cubics whose roots sum to zero and which have 1 as a root. Since any cubic can be transformed into an p_λ or into z^3 by an affine change of variable and multiplication by a constant, analyzing Schröder's method for a general cubic reduces essentially to analyzing it for the p_λ's.

Each point $\lambda = \mathrm{Re}(\lambda) + i\,\mathrm{Im}(\lambda)$ represents a dynamical system with its own fixed points, possible attracting cycles and Julia sets. There are regions in the λ-parameter space where attracting periodic cycles exist in addition to the attracting fixed points associated with the zeros of p_λ. Extra fixed points corresponding to the roots of Eq. (4), shown to be repelling for $\lambda = 1$, may become attracting in regions of the λ-space. To detect the existence of attracting cycles which could interfere with the Schröder search for the z_i^*, we observe the orbits of the free critical points of the S_σ functions.

The free critical points $c_i, i = 1, 2, \ldots, \sigma - 1$ for the first three S_σ functions associated with p_λ can be computed by Eq. (5) and are given below:

$\sigma = 2$, $c_1 = 0$,
$\sigma = 3$, $c_{1,2} = \pm\sqrt{(\lambda - 1)/15}$,
$\sigma = 4$, $c_{1,2} = \pm\sqrt{(\lambda - 1)/6}$, $\quad c_3 = 0$.

The free critical points for the first ten S_σ functions associated with p_λ are presented in [5].

The dynamics of each Schröder map S_σ on the extended complex parameter space was studied in much the same way as described in Section 5 of this paper and in Subsection 5.2 of [5], except that the region of the complex λ-plane was represented by a circle grid. The grid point in λ-space was colored accordingly: blue for convergence to z_1^*, red for convergence to z_2^* and green for convergence to z_3^*. The resulting black areas represent regions in parameter space for which additional attracting cycles existed. The corresponding parameter space maps for the critical points $c_{i+1} = -c_i$ are obtained by a reflection about the real λ-axis. For the Figures 5, 7(a) and 7(b) the angles were, in the x-direction, $O°$ and, in the y-direction, $-9O°$. The overflow parameter was $1E30$.

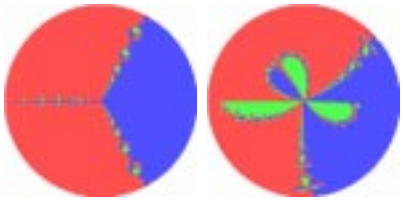

(a) (b)

Figure 5: Iteration schemes for the one-parameter family of cubic polynomials p_λ; (a) S_2 method, (b) S_3 method.

Case 1. $\sigma = 2$: Figure 5(a) represents regions in parameter space for which the critical point c_1 is attracted to z_i^*. Figure 6(a) is an enlargement of a region in Figure 5(a), but located on the dark side of this sphere.

Case 2. $\sigma = 3$: Figure 5(b) represents regions in parameter space for which the critical point c_1 is

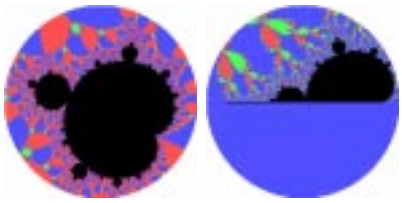

(a) (b)

Figure 6: Magnifications of Figures 6(a) and 6(b) revealing Mandelbrot sets for the S_2 and S_3 methods, respectively.

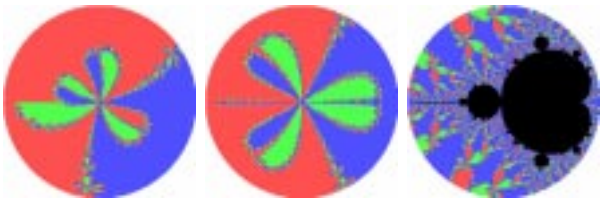

(a) (b) (c)

Figure 7: (a), (b) S_4 iteration scheme for the one-parameter family of cubic polynomials p_λ. (c) A magnification of a region of Figure (b) revealing a Mandelbrot set for the S_4 method.

attracted to z_i^*. Figure 6(b) is an enlargement of a region in Figure 5(b).

Case 3. $\sigma = 4$: Figures 7(a) and (b) represent regions in parameter space for which the critical points c_1 and c_3, respectively, are attracted to z_i^*. Figure 7(c) is an enlargement of a region in Figure 7(b) showing a Mandelbrot-like set associated with c_3.

Because the black shapes that we discovered in the λ-parameter space exhibit the morphology and the classical characteristics of Mandelbrot sets, it comes in a non-surprising fashion the following

Definition 1 The Mandelbrot set *associated with the Schröder function S_σ for the cubic polynomials p_λ is the set*

$$\mathcal{M}_\sigma(\lambda) = \{\lambda \in \mathbb{C} : \textit{ there exist attracting } k\textit{-cycles}, \; k = 1, 2, \ldots, \textit{ for } S_\sigma \textit{ other than the roots } z_i^* \textit{ of } p_\lambda(z) = 0\}.$$

References

[1] K.–H. Becker and M. Dörfler, *Dynamische Systeme und Fraktale: Computergrafische Experimente mit Pascal*, 3. Auflage, Vieweg, 1989.

[2] J. H. Curry, L. Garnett and D. R. Sullivan, On the iteration of a rational function: Computer experiments with Newton's method, *Communications in Mathematical Physics*, Vol. 91, No. 2, 1983, pp. 267–277.

[3] V. Drakopoulos, On the additional fixed points of Schröder iteration functions associated with a one-parameter family of cubic polynomials, *Computers & Graphics*, Vol. 22, No. 5, 1998, pp. 629–634.

[4] V. Drakopoulos and A. Böhm, Basins of attraction and Julia sets of Schröder iteration functions, in T. Bountis and Sp. Pnevmatikos (eds), *Order and chaos in nonlinear dynamic systems*, Vol. IV, Pnevmatikos, 1998.

[5] V. Drakopoulos, N. Argyropoulos and A. Böhm, Generalized computation of Schröder iteration functions to motivate families of Julia and Mandelbrot-like sets, *SIAM Journal on Numerical Analysis*, Vol. 36, No. 2, 1999, pp. 417–435.

[6] M. P. Fatou, *Sur les équations fonctionelles*, Bulletin de la Société Mathématique de France, Vol. 47, 1919, pp. 161–271; Vol. 48, 1920, pp. 33–94, 208–314.

[7] P. Henrici, *Applied and computational complex analysis*, Vol. 1, Wiley, 1974.

[8] G. Julia, Mémoire sur l'itération des fonctions rationelles, *Journal de Mathématiques Pures et Appliquées*, Vol. 8, 1918, pp. 47–245.

[9] E. Schröder, Über unendlich viele Algorithmen zur Auflösung der Gleichungen, *Mathematische Annalen*, Vol. 2, 1870, pp. 317–365.